

Adversarial Item Promotion: Vulnerabilities at the Core of Top-N Recommenders that Use Images to Address Cold Start

ZHUORAN LIU and MARTHA LARSON, Radboud University, Netherlands

E-commerce platforms provide their customers with ranked lists of recommended items matching the customers' preferences. Merchants on e-commerce platforms would like their items to appear as high as possible in the top-N of these ranked lists. In this paper, we demonstrate how unscrupulous merchants can create item images that artificially promote their products, improving their rankings. Recommender systems that use images to address the cold start problem are vulnerable to this security risk. We describe a new type of attack, *Adversarial Item Promotion* (AIP), that strikes directly at the core of Top-N recommenders: the ranking mechanism itself. Existing work on adversarial images in recommender systems investigates the implications of conventional attacks, which target deep learning classifiers. In contrast, our AIP attacks are embedding attacks that seek to push features representations in a way that fools the ranker (not a classifier) and directly lead to item promotion. We introduce three AIP attacks *insider attack*, *expert attack*, and *semantic attack*, which are defined with respect to three successively more realistic attack models. Our experiments evaluate the danger of these attacks when mounted against three representative visually-aware recommender algorithms in a framework that uses images to address cold start. We also evaluate two common defenses against adversarial images in the classification scenario and show that these simple defenses do not eliminate the danger of AIP attacks. In sum, we show that using images to address cold start opens recommender systems to potential threats with clear practical implications. To facilitate future research, we release an implementation of our attacks and defenses, which allows reproduction and extension.

1 INTRODUCTION

Image content is considered a promising means to address the cold start problem of recommender systems [15, 18, 23]. In this paper, we show that the use of image content for cold start opens recommenders to vulnerabilities in the form of *adversarial items*. Adversarial examples are deliberately designed samples that cause a machine learning system to make mistakes. In the computer vision community, adversarial images have been shown to be a security issue for classification systems [3, 32]. Here, we demonstrate that there are actually vulnerabilities that go beyond classification and exist at the core of the recommender system, interfering with the ranking mechanism. There has been a limited amount of previous work on the danger of adversarial images for recommender systems [11, 33]. However, until now, this work have focused on classification-related issues or adversarial training for general performance improvement. The main contribution of this paper is to reveal the vulnerabilities that arise when images are used to address cold start in recommender systems and to show that simple solutions will not solve them.

In the recommender system community, a sizeable amount of research has been devoted to the security and robustness of recommender system algorithms [5, 8, 19, 24, 25]. Most work, however, focuses on vulnerabilities related to user profiles. Early work looked at *shilling* [19], which uses fake users. Shilling was later generalized to *profile injection attacks* [24]. In our work, in contrast, we are looking at attackers who have the power to manipulate items directly, and, specifically, to choose item images. In other words, instead of looking at profile injection attacks we are looking at an *item representation attacks*. Concretely, the risk of such attacks presents itself in the case of e-commerce platforms that sell the items of individual merchants, e.g., e-commerce or customer to customer (C2C) marketplaces. The merchants create their own item description, including images. We show that if such merchants act unscrupulously they can artificially promote their items and compromise the security of the recommender system .

Authors' address: Zhuoran Liu, z.liu@cs.ru.nl; Martha Larson, m.larson@cs.ru.nl, Radboud University, Netherlands.

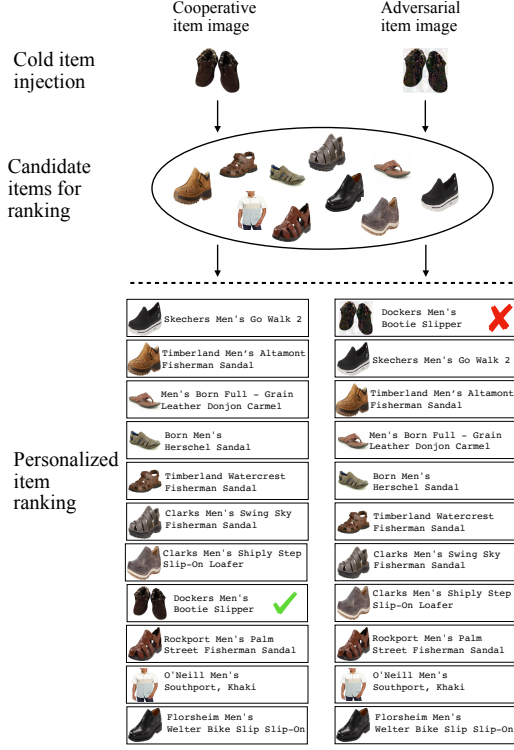


Fig. 1. The cooperative cold item image and its corresponding adversarial cold item image are shown at the top. After injecting the cold item into the candidate set, which is generated by a first-stage ranker (here, BPR), a visually-aware second-stage ranker (here, DVBPR) ranks the cooperative item low and the adversarial item high in the final personalized ranking of items. (This diagram shows a real example. The adversarial item image is generated by our INSA attack with $\epsilon = 32$ and epoch = 5 explained in detail in Section 4.1).

Notation	Explanation
\mathcal{U}, \mathcal{I}	user and item set
$\mathcal{I}_{\text{cold}}$	cold item set
θ_u, θ_i	content embedding for user and item
y_u, y_i	latent embedding for user and item
Φ_f, Φ_g	neural network for feature extraction embedding
$\mathbf{X}_i \in \mathbb{R}^{224 \times 224 \times 3}$	product image for item i
$\mathbf{X}_{\text{hook}} \in \mathbb{R}^{224 \times 224 \times 3}$	hook item
δ	adversarial image perturbations
ϵ	restriction threshold of L_∞ norm
$p_{u,i}$	preference prediction for user-item pair (u, i)
$\Delta_{u,i}$	prediction shift for user-item pair (u, i)
Δ_i	average prediction shift for item i
$\mathbf{X}_i^{\text{adv}} \in \mathbb{R}^{224 \times 224 \times 3}$	adversarial product image for item i

Table 1. Notations used in this paper.

Figure 1 illustrates the mechanics of the attack that we consider in this paper, called an *Adversarial Item Promotion* (AIP) attack. On the left, we see personalized item ranking for a user when the recommender system is *not* under attack (i.e., the cold start item is a “cooperative item”). On the right, we see the ranking when the recommender system is under attack by an unscrupulous merchant, who has used a manipulated image in an item representation (i.e., the cold start item is an “adversarial item”). This cold item setup assumes that the recommender system platform wants to add a certain number of cold items to the personalized ranked lists of users in order to allow the items to start accumulating interactions. In Figure 1, we see the case of a single cold item and a single user. A set of “candidate items for ranking” for that user has been selected using a conventional personalized Top-N recommender. Then the cold item is injected into that set. Finally, a visually-aware personalized Top-N recommender is used to rank the candidate item set before it is presented to the user. In Figure 1 (left) we see that in the case of the cooperative image, the cold item

lands somewhere in the ranked list, but probably not at the top. In contrast, in Figure 1 (right) we see that in the case of the adversarial image, the cold item lands at the top of the personalized item ranking.

The overall impact of the attack depends on the accumulated effect of the attack over all users, and not just a single instance of the attack, which is shown in Figure 1. Note that the final rank position of the cooperative vs. adversarial item will be different for each instance of the attack. However, in general, if the adversarial item of an unscrupulous merchant lands consistently farther towards the top of users’ personalized recommendation lists than it deserves to, then, at large scale, the merchant will accrue considerable benefit. If we consider that a certain portion of the merchant’s sales is correlated with rank-position, then the revenue of the merchant will increase. Also, the number of interactions that the item receives will also increase. This means that the impact of the adversarial image is effectively translated from the visual modality into the user-item interaction data, where it can increase the chance of the item to be selected by the first-stage recommender. We do not quantify the rewards here, but we mention them because they provide strong motivation for an unscrupulous merchant to invest time and effort in an AIP attack.

It is important to understand that the potential danger of AIP attacks extends beyond the specific cold-start setup that we use in this paper. We choose a two-stage recommender, since they are used in industry [10, 34]. Also, with the two-stage recommender we ensure that the adversarial item is competing against items that are already very relevant to the user. This means that it is actually more difficult to promote an adversarial item in a two stage setup then it would be if the injection occurred in a single-stage setup. In other words, our setup is realistic and mounting the attack is non-trivial and has meaningful implications for real-world recommenders. We choose to focus on the cold-start problem because of its importance for recommender systems. However, there is also another reason. A straightforward, practical approach to blocking adversarial image promotion attacks on non cold start items is to prevent merchants from being able to change images once their items have started to accumulate interactions. Cold start is the most important moment of opportunity for a merchant to introduce an adversarial image into a representation. Every item starts in some way cold, and the issue particularly extreme in C2C marketplaces selling many unique items. In this paper, we experimentally demonstrate the vulnerability of visually-aware recommenders. We also provide experimental evidence that blocking AIP attacks in cases of item cold start requires more than a simple defense. In short, the issues we point out here require further attention from the research community.

We follow the standard procedure for security research. First, we specify a framework including the types of attacks expected (attack models), the systems to be attacked, and a means of measuring the strength of attacks. Then, we propose attacks for each attack model and evaluate their success. The systems that we attack are representative of visually-aware recommender systems, i.e., a visual feature-based similarity model (AlexRank), a Collaborative-Filtering (CF) model leveraging visual features (VBPR), and state-of-the-art learning-based neural model (DVPBR). This paper makes the following contributions:

- We point out that the impact of adversarial images on recommender systems is not just a straightforward translation of adversarial images from the computer vision, and may be more dangerous than we realize.
- We propose three Adversarial Item Promotion (AIP) attacks in a cold item scenario corresponding to three different levels of knowledge and validate the effectiveness of proposed attacks on two real-world data sets.
- We show that the problem of AIP attacks is a serious one. Our experiments demonstrate that two defenses commonly used for the classification problem will not eliminate the danger of AIP attacks.
- We release an implementation of our attacks and defenses that allows for testing and extension¹.

¹Our code is available at: <https://github.com/liuzrc/AIP>

2 RELATED WORK

2.1 Robustness of recommender system

The robustness of recommender systems has been widely studied in the past [5, 8, 19, 24, 25]. Mahony *et al.* [25] introduce the definition of recommender system robustness and present several attacks to identify characteristics that influence robustness. Lam and Riedl [19] explore shilling attacks in recommend systems by evaluating the recommendation performance under different scenarios. In particular, they find that new or obscure items are more especially susceptible to attack, and they suggest that obtaining ratings from a trusted source for these items could make them less vulnerable. Mobasher *et al.* [24] propose a formal framework to characterize different recommender system attacks, and they also propose an approach to detect attack profiles. In [24] and [5], evaluation metrics, e.g., hit rate for item and prediction shift, for robustness of recommender system are discussed. Christakopoulou and Banerjee [8] propose an automatic generative approach to generate fake user profiles to mount profile injection attack. Our “item representation attack” is distinct from a “profile injection attack”, but both two kinds of attacks have similar impact results, namely, pushing items that have been targeted for promotion.

2.2 Visually-aware recommender system

Previously, visually-aware recommender systems are systems that rely on visual content, usually in combination with user-item interactions. Conventionally, visually-aware recommenders are developed on the basis of image retrieval techniques. Given a query image, Kalantidis *et al.* [17] classify segmentation parts and retrieve visually similar items within each of the predicted classes. Jagadeesh *et al.* [16] gather a large-scale dataset, Fashion-136K, with detailed annotations and propose several retrieval-based approaches to recommend the missing part based on query image. Going a step further, IBR [23] models human notions of similarity by considering alternative or complementary items.

Beyond similarity-based recommendation approaches, fashion or style characteristics approaches also play an important role. Simo-Serra *et al.* [31] models how fashionable a person looks in an image, and it made fashion recommendations based on the calculated fashionability scores. Combining the existing visual feature-based algorithms and collaborative filtering approaches, VBPR [15] is devised to leverage both user feedback and visual features. Instead of optimizing the matrix-factorization model in VBPR with pre-trained features, DVBPR [18] proposes an end-to-end CNN-based framework and achieves state of the art results on several fashion recommendation data sets.

Apart from recommender systems that rely on visual information, several multi-modal approaches that also use other auxiliary information are proposed in both academia and industry [4, 36, 37]. The popularity of modeling heterogeneous information in recommender systems makes it crucial to re-consider the system robustness with respect to auxiliary information sources.

2.3 Adversarial examples in machine learning

Adversarial examples are data samples that are deliberately designed in order to mislead machine learning algorithms. Adversarial modifications strive to be imperceptible to humans, e.g., in images [32] and in audio [7]. For recommender systems user acceptance, and imperceptibility is not the key factor. We address this point by proposing a semantic approach which circumvents the needs for perturbations.

A limited amount of work, as mentioned above, has addressed adversarial images for recommender systems. Some work has focused on leveraging adversarial images to improve recommendation performance. Tang *et al.* [33] consider the robustness of recommender systems against adversarial representation perturbations with the goal of improving

the recommendation with adversarial training. In contrast to [33], who focus on increasing general recommendation performance, our goal is to investigate security vulnerabilities of recommender systems.

The work most closely related to our own [11] looks only at classification-based issues. Di Noia *et al.* [11] propose a new metric Category Hit Ratio and use two classification-based adversarial attacks to evaluate two visually-aware recommender systems. In contrast to [11], we show that the problem of adversarial examples in recommender system does not reduce to the problem of adversarial examples in classification.

3 FRAMEWORK

In this section, we introduce the framework in which the attack models are developed and evaluated. Figure 2 gives the overview of the setup. As previously discussed, we use a two-stage approach. We use the first-stage recommender to generate a personalized set of candidate items. For this purpose, we choose Bayesian Personalized Ranking (BPR) [28], a representative CF model that is trained on the user-item interaction data. We use the visually aware second-stage recommender to make a comparison between the cold start of a cooperative item and an adversarial item.

Section 3.1 presents the three attack models we investigate in this paper (the basis for creating three specific AIP attacks, INSA, EXPA, and SEMA, explained in Section 4). Section 3.2 explains the three visually-aware recommenders that we attack. Finally, the evaluation of the attacks is explained in more detail in Section 3.3. Frequently used notations are summarized in Table 1.

	General Knowledge	Visual feature extraction model	Embeddings
High-knowledge attack model (corresponds to INSA cf. Section 4.1)			×
Medium-knowledge attack model (corresponds to EXPA cf. Section 4.2)	×	×	
Low-knowledge attack model (corresponds to SEMA cf. Section 4.3)	×		

Table 2. The attack models used to develop our AIP attacks.

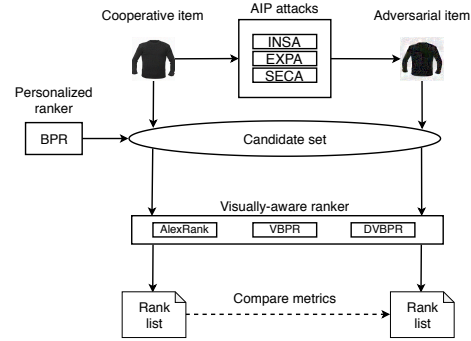


Fig. 2. Setup for attack and attack evaluation.

3.1 Attack Models

We define three attack model following the three dimensions relevant for trustworthy recommender systems [24]. The *Intent* dimension captures the objective of the attacker. All our models use ‘push’ intent, i.e., attackers are merchants who want their items promoted to higher ranks in users’ personalized recommendation lists. The *Knowledge* dimension captures how much information that the attacker has about the system being attacked. Our three attack models correspond to three different levels of knowledge: high, medium, and low. The *Scale* dimension captures the scope of the impact on the recommender system. In all our attack models, we assume an attack with minimum scale that is not likely to be noticed. It is clear that the harm inflicted by the attack will increase with attack size.

Table 2 summarizes our attack models in terms of the level of knowledge involved. For our high-knowledge attack model we assume that the attacker is an insider at the recommender system platform and has access to the user

embeddings of the trained recommender model. This scenario is not particularly realistic, but it is important because it demonstrates an upper bound for the potential damage that can be inflicted by an AIP attack.

The medium- and low-knowledge attack models are more realistic and assume that the attacker has general knowledge of the market in which the recommender system operates. In particular, the attacker must be able to identify (by observing sales trends or advertising) at least one item that sells well on the platform. We refer to this item as a *hook* item. The attack is strongest when the hook item image is an image used by the recommender, but could also be an image of the item acquired elsewhere. As will be explained in Section 4, the adversarial item will use the hook item to pull itself up in the ranked list. In the medium-knowledge attack model, in addition to general knowledge, the attacker must have access to the pre-trained visual feature extractor used by the visually-aware recommender systems. Recommender systems leveraging pre-trained visual feature extractor are prevalent in both academic research and industry, e.g., [13, 15, 20, 23, 27, 30]. These models are often released as publicly available resources.

In general, we assume that the recommender system platform is so large and the turnover of items so fast that it is impossible to manually vet all of the images representing items. We consider this assumption reasonable given the known difficulty of filtering item collections for banned or unsafe products [2]. We also assume that users are relatively insensitive to image quality. Computer vision research, as previously mentions, tends to focus on ensuring that image manipulations are as imperceptible as possible. Here, we only need to achieve acceptability: the item must be clearly discernible in the adversarial image.

3.2 Visually-aware Recommender Systems

In this section, we introduce the three representative visually-aware recommender systems that we will attack in our experiments. In particular, we introduce the visual feature-based similarity model (AlexRank), the CF model leveraging visual features (VBPR), and state-of-the-art learning-based approach (DVBPR). We chose these recommenders because they represent the three types of commonly used visually-aware recommender systems.

3.2.1 AlexRank. Image content retrieval-based recommendation is a nearest neighbour approach that ranks items by visual similarity of product images. Given an image of item i , the average Euclidean distance between item i and all items that user u has interacted with is calculated, so smaller distance resembles higher preference prediction. Equation 1 show the calculation of similarity predictor:

$$p_{u,i} = \sum_{j \in D_u} \frac{\|\Phi_f(X_i) - \Phi_f(X_j)\|^2}{|D_u|}, \quad (1)$$

where D_u is the set of items that user u has interacted with, and X_i, X_j represents the image of item i and j . Φ_f is the pre-trained model for image feature extraction.

3.2.2 VBPR. Improved from BPR [28], VBPR [15] incorporates visual features into BPR model. By leveraging the image features of pre-trained CNN models, VBPR improves the performance of BPR. The preference prediction of VBPR is described in Equation 2:

$$p_{u,i} = \alpha + \beta_u + \beta_i + \gamma_u^T \gamma_i + \theta_u^T (E \Phi_f(X_i)), \quad (2)$$

where θ_u is the user content embedding, and E is the parameter for visual feature. $\Phi_f(X_i)$ represents the visual feature of item X_i from pre-trained model Φ_f .

3.2.3 DVBPR. Extended from VBPR, DVBPR [18] is a concise end-to-end model whose visual feature extractor is trained directly in a pair-wise manner. DVBPR achieves the state-of-the-art performance on several data sets for visually-aware recommendations. The preference prediction of DVBPR is described in Equation 3:

$$p_{u,i} = \theta_u^T \Phi_e(\mathbf{X}_i), \quad (3)$$

where θ_u is the user content embedding, and $\Phi_e(\mathbf{X}_i)$ is the item content embedding where the CNN model Φ_e is trained directly in a pair-wise manner.

3.3 Evaluation

We evaluate our attacks by measuring their ability to raise the rank of adversarial cold-start items such that they are promoted above cooperative cold start items in users' recommended item lists. This corresponds to the 'push' intent of our attack models, cf. Section 3.1. The strength of the push is related to the *integrity* dimension of machine learning security security [1]. The change in rank of cold-start items is measured by the prediction shift and the change in hit rate (HR@N), following the evaluation metrics for top-N recommender system robustness [24] and [5]. Equation 4 defines the average prediction shift Δ_i for item i and also the mean average prediction shift for a set of cold items Δ_{cold} . $p'_{u,i}$ is the post-attack predictor score and $p_{u,i}$ is the original predictor score for item i .

$$\Delta_i = \sum_{u \in \mathcal{U}} \frac{(p'_{u,i} - p_{u,i})}{|\mathcal{U}|} \quad \Delta_{\text{cold}} = \sum_{i \in \mathcal{I}_{\text{cold}}} \frac{\Delta_i}{|\mathcal{I}_{\text{cold}}|}, \quad (4)$$

Equation 5 defines the average hit rate for item i ($HR_i@N$) in terms of the hit rate of item i for user u ($H_{u,i}@N$). The mean average hit rate for cold items (HR_{cold}) averages $HR_i@N$ over all cold items that are tested. $\Delta_{\text{test}}^{HR@N}$ is the change in hit rate.

$$HR_i@N = \sum_{u \in \mathcal{U}} \frac{H_{u,i}@N}{|\mathcal{U}|} \quad HR_{\text{cold}}@N = \sum_{i \in \mathcal{I}_{\text{cold}}} \frac{HR_i@N}{|\mathcal{I}_{\text{cold}}|} \quad \Delta_{\text{cold}}^{HR@N} = \sum_{i \in \mathcal{I}_{\text{cold}}} \frac{HR_i^{\text{adv}}@N - HR_i^{\text{coop}}@N}{|\mathcal{I}_{\text{cold}}|} \quad (5)$$

In addition to the *integrity* dimension, the *availability* dimension is also important, since it relates to whether the recommender system remains useful to merchants and customers while under attack. We measure availability using the test items (which are defined by the data set releases). Specifically, we calculate the change in hit rate when a test item is in a candidate set with a collaborative cold item and when the same test item is in a candidate set with an adversarial cold item.

4 ADVERSARIAL ITEM PROMOTION ATTACKS

In this section, we introduce three adversarial item promotion (AIP) attacks corresponding to the three attack models previously introduced in Section 3.1.

4.1 Insider Attack (INSA)

The high-knowledge attack model assumes the attacker has insider access to the user embeddings of the trained model (see Section 3.1). Recall that most visually-aware recommender systems model the visual content embedding together with user content embedding (cf. Section 3.2). For instance, in DVBPR, the inner product of user embedding θ_u and item embedding $\Phi_e(\mathbf{X}_i)$ represents the preference of user u on item i . We propose an insider attack (INSA) in which the attacker uses the embeddings to create an adversarial image for the adversarial item. Specifically, the embeddings

are used to generate perturbations δ that are added to the original image in order to create the adversarial image. The perturbations are optimized such that the strength of preference for the item is maximized over all user profiles. Formally, given a product image \mathbf{x}_i of item i , we optimize perturbations δ to increase the preference $p_{u,i}$ of all users on item i . The optimization process is described in Equation 6:

$$\delta \leftarrow \underset{\delta}{\operatorname{argmax}} \sum_{u \in \mathcal{U}} \exp(\theta_u^T \Phi(\mathbf{x}_i + \delta)), \quad (6)$$

where θ_u is the user content embedding. The optimization can be implemented by mini-batch gradient descent, and it stops until certain conditions are met, e.g., it reaches certain number of iterations.

4.2 Expert Attack (EXPA)

The medium-knowledge attack model assumes that the attacker can select a hook (i.e., popular) item and also has access to the visual feature extraction model (see Section 3.1). We propose an expert attack (EXPA) in which the attacker uses the hook item to mark the region of item space to which the adversarial item should be moved. Specifically, the EXPA attack generates perturbations added to the cooperative item in order to create the adversarial item by decreasing the representation distance to the hook item.

Formally, generating an adversarial item image by EXPA is described in Equation 7:

$$\delta \leftarrow \underset{\delta}{\operatorname{argmin}} \|\Phi(\mathbf{x}'_i + \delta) - \Phi(\mathbf{x}^{\text{hook}})\|_2, \quad (7)$$

where Φ_f is the feature extraction model. The EXPA attack leverages the same mechanism as the targeted visual feature attack proposed by [29]. The novelty of EXPA is its use of a hook image that moves the adversarial image in image space in a way that makes it rise in personalized recommendation lists. Note that the hook image itself is not necessarily present in candidate set, which is selected by BPR, and thereby also not in the recommendation lists.

Algorithm 1 describes the process to generate adversarial product images with INSA and EXPA. \mathbf{X}_i is the original image of cold item, and \mathbf{X}^{hook} is the hook item. Φ is the neural network that extracts embeddings or features from the image content. Our aim is to find perturbations δ that could increase the personalized preference predictions by optimization through all user content embeddings (INSA) or targeting a hook item (EXPA). At the same time, we also need to restrict the magnitude of δ with respect to L_∞ norm to make these perturbations imperceptible. The resulting adversarial image \mathbf{X}^{adv} is the summation of the original image and the clipped perturbations.

4.3 Semantic Attack (SEMA)

The low-knowledge attack model assume nothing beyond general knowledge needed to choose hook items (see Section 3.1). We propose a semantic attack (SEMA) uses the semantic content of the image, i.e., what is shown in the image, in order to achieve the promotion of items. The attack differs considerably from INSA and EXPA, which add perturbations to existing images without changing what the images depict.

Figure 3 (c) illustrates the semantic attack that we will test here, which we call composition semantic attack (c-SEMA). With c-SEMA, the attacker creates an adversarial image by editing the original image into the hook item image as an inset. Here, the c-SEMA attack is promoting a pair of shoes and the hook item is the jeans. A text (here, "match your jeans with") can be included to contribute to the impression that the composite image is a standard attempt to raise the interest of potential customers.

Algorithm 1 Adversarial Item Promotion Attack**Input:**X: cold item image, X^{hook} : hook item image δ : adversarial perturbations, ϵ : L_∞ norm bound Φ : neural network, θ : user content embedding K : number of iterations**Output:** X^{adv} : adversarial product image

- 1: Initialize $x'_0 \leftarrow X$, $x^t \leftarrow X^{\text{hook}}$, $\delta \leftarrow 0$
- 2: **for** $k \leftarrow 1$ to K **do**
- 3: Update δ by Eq. (6)/Eq. (7) for INSA/EXPA attack ▷ Update δ by gradients
- 4: $\delta \leftarrow \text{clip}(\delta, -\epsilon, \epsilon)$ ▷ Make sure that the magnitude of perturbations are in pre-defined L_∞ norm range
- 5: $x'_k \leftarrow x'_{k-1} + \delta$
- 6: $x'_k \leftarrow \text{clip}(x' + \delta_k, 0, 1)$
- 7: **end for**
- 8: $x'_k \leftarrow \text{quantize}(x'_k)$ ▷ Ensure x'_k is valid
- 9: **return** $X^{\text{adv}} \leftarrow x'_k$ is the adversarial product image that targets X^{hook}



Fig. 3. Examples of adversarial item images by different approaches. INSA attack is based on Equation 6. EXPA, c-SEMA and n-SEMA select a popular item, i.e., Levi's 501 jeans, as the hook item. c-SEMA applies simple co-depiction approach, and n-SEMA incorporates the target item in a more natural way.

Figure 3 (d) shows another type of semantic attack, which we call natural semantic attack (n-SEMA). Here, the integration of the hook item is natural. n-SEMA images can be created in a photo studio or a professional photo editor. We do not test them here, since creation is time consuming and we are using a cold item set of 1000 images. However, an unscrupulous merchant would have the incentive to invest the time to create n-SEMA images. One highly successful adversarial item image could already lead to increased buyers and increased profit.

The semantic attack is particularly interesting for two reasons. SEMA achieves the change in image embeddings needed to push an adversarial image close to a hook image in image space by manipulating the depicted content of the image. First, this means that there are no limits on the quality of a SEMA adversarial image. Contrast c-SEMA and n-SEMA in Figure 3(c) and (d) with the INSA and EXPA photos in Figure 3(a) and (b). The item is visible in the image, and consumers who decide to purchase the product will not find that they have been misled. However, the images are not crisp, and contain artifacts. Second, the impact of a SEMA image attack is not dependent on the algorithm used by the recommender systems. In fact, SEMA images can effectively attack any recommender system using visual features, and not just systems using neural embeddings as studied here.

Table 3. Statistics of the data sets

	#Users	#Items	#Interactions
Amazon Men	34244	110636	254870
Tradesy.com	33864	326393	655409

5 EXPERIMENTS

In this section, we first introduce data set in Section 5.1 and implementation details in Section 5.2. Then, we carry out experimental analysis on two real-world data sets and investigate the influence of hyper-parameter selections in Section 5.3. Finally, we evaluate two defenses against AIP attacks in Section 5.4.

5.1 Data

5.1.1 Data sets. We perform our experiments on two data sets: Men’s Clothing in Amazon.com and Tradesy.com, which are publicly available and widely used in visually-aware recommender system research. The statistics of the two data sets are described in Table 3. Men’s Clothing category is an important subset of Amazon.com data set, where the effectiveness of visual features have been validated in many works [15, 18, 23]. Tradesy.com is a c2c second-hand clothing trading website where users can buy and sell fashion items. Its business mode also makes visually-aware cold item recommendation crucial, because its ‘one-off’ characteristics. For both datasets, one descriptive image is available for each item, and we follow the protocol of [18] and treat users’s review histories as implicit feedback. For each user, one item is selected among all interacted items as the test item, so we have the same number of test items as the number of users.

5.1.2 Cold item selection. To validate the effectiveness of the attacks in cold start scenario, in each of Amazon Men and Tradesy.com data sets, we randomly select 1000 cold items that users have never interacted with and leave them out as the external cold item test set. These cold items are excluded from the training process. Later, they are injected as cold items to the candidate item set before feeding into the visually-aware ranker.

5.2 Implementation

In the first stage, we use BPR to generate a candidate set of top 1000 items that are selected by personalized preference ranking. Here we use a set, which means that the original rank order is not taken into account by the visually-aware recommender algorithm. Then we inject the test item in the top 1000 candidate set and get a set of 1001 items for each user. To compare before and after the attack, we inject one cooperative cold item or its corresponding adversarial item in the candidate set. For each cold item, we have two set of 1002 items, which includes one test item and one cooperative item (or one adversarial cold item). We use three different visual ranking models, AlexRank, VBPR, and DVBPR (see Section 3.2), to rank the 1002 items and evaluate with respect to both integrity and availability (see Section 3.3).

5.2.1 Model Training. We implement BPR, AlexRank, VBPR, and DVBPR in PyTorch [26]. For the first stage model BPR, we set the number of factors 64. Stochastic Gradient Descent (SGD) is used to optimize BPR with learning rate 0.01 for Amazon Men and 0.5 for Tradesy.com, where weight decay for L2 penalty is set to 0.001 on both data sets. A grid search of learning rate in {0.1, 0.01, 0.001, 0.005} and weight decay in {0.001, 0.0001, 0.0001} is conducted for both VBPR and DVBPR to select hyper-parameters, and we select the model with best validation performance.

Table 4. Absolute mean average prediction shifts of adversarial cold items $|\Delta_{\text{cold}}|$, where \uparrow represents positive prediction shift (rank increased) and \downarrow represents negative prediction shift (rank decreased). Positive shift is a successful attack.

	BPR + AlexRank (dim=2048)			BPR + VBPR (#factors=100)			BPR + DVBPR (#factors=100)		
	INSA	EXPA	c-SEMA	INSA	EXPA	c-SEMA	INSA	EXPA	c-SEMA
Amazon Men	$\uparrow 16.13$	$\uparrow 15.94$	$\uparrow 11.1$	$\uparrow 3.27$	$\uparrow 3.16$	$\uparrow 0.88$	$\uparrow 13.54$	$\uparrow 4.80$	$\uparrow 4.82$
Tradesy.com	$\uparrow 26.89$	$\downarrow 0.67$	$\downarrow 3.44$	$\downarrow 0.79$	$\uparrow 1.60$	$\uparrow 1.45$	$\uparrow 3.64$	$\uparrow 1.89$	$\uparrow 1.19$

5.2.2 Adversarial attacks. If not specially mentioned in our paper, the maximal size of perturbations ϵ for AIP attacks is set to 32. In INSA, the number of epochs is set as 5 to control the attacking time, and our implementation takes about 4 hours to generate 1000 adversarial item images on a single GPU. We use the Adam optimizer with the learning rate of 0.001 for DVBPR and 0.0001 for both VBPR and AlexRank. In EXPA, the hook items are “Levi’s Men’s 501 Original Fit Jean” in Amazon Men and a gray coat in Tradesy.com. These two products are most commonly interacted items in training data of these two data sets. Recall, however, that hooks can be chosen without direct access to interaction statistics. We use a Adam optimizer with a learning rate of 0.01, and the number of iterations is set as 5000.

5.3 Experimental Results

In this section, we mount AIP attacks and evaluate their effects within the framework described in Section 3.

5.3.1 Attack Evaluation. Table 4 shows the absolute mean average prediction shift Δ_{cold} for cold-start items. The upwards arrow represents a positive prediction shift, meaning that the attack successfully promoted the item. We see that for nearly all combinations of AIP attack and visually-aware recommender system the attack is successful. The high-knowledge attack INSA achieves a larger shift than EXPA and c-SEMA. c-SEMA is surprisingly successful given the very minimal amount of knowledge that it requires. Note that it is only meaningful to compare the size of the prediction shift for the same recommender system and the same data set.

Table 5 shows the mean average hit rate $HR_{\text{cold}}@N$ for cold items and average hit rate $HR_{\text{test}}@N$ for test items, providing more insight into the attacks. The first row for each data set reports the hit rate of the original test items in the case that no adversarial items have been added to the candidate set. The second row reports the hit rate of the cooperative cold items when they are added to the candidate set. The rest of the rows report the hit rate of the test items added to candidate set containing an adversarial cold items (“Test with” rows) and the hit rate of adversarial cold items that have been created by the different attacks. Recall that measurements made on cold items reflect impact of the attack on integrity and measurements made with test items reflect the impact on availability.

It can be observed that all AIP attacks are generally effective. For INSA, the attack is dramatic: On average, approximately 24660 users will find the adversarial cold item in top-5 ranking on Amazon Men data set, and the number before the attack is 35. Since INSA uses the most knowledge, it is not surprising that it is the most effective attack. However, even with much less available knowledge, both EXPA and c-SEMA pose a serious threat. For example, on Amazon Men data set, c-SEMA pushes the cold item to the hit rate level of a popular hook item.

Another key observation is that although the goal of an AIP attack is to push adversarial items, the attack also influences the performance of other items (cf. “Test with” rows). This means that unscrupulous merchants using AIP attacks promote their own items at the measurable expense of other items, which at scale can impeded the functioning of the entire recommender system.

Table 5. Average HR@N of test item and cooperative (adversarial) cold item in AlexRank, VBPR and DVBPR. Three attacks, INSA ($\epsilon = 32$), EXPA ($\epsilon = 32$) and c-SEMA, are evaluated on Amazon Men and Tradesy.com data sets.

	AlexRank (dim=2048)			VBPR (#factors=100)			DVBPR (#factors=100)		
	HR@N			HR@N			HR@N		
	N = 5	N = 10	N = 20	N = 5	N = 10	N = 20	N = 5	N = 10	N = 20
Amazon Men									
Original test	0.0195	0.0372	0.0681	0.0191	0.0373	0.0691	0.0187	0.0461	0.0808
Cooperative cold	0.0010	0.0023	0.0053	0.0017	0.0037	0.0082	0.0011	0.0038	0.0092
Test with INSA	0.0140	0.0423	0.0784	0.0190	0.0375	0.0676	0.0170	0.0352	0.0659
INSA adv cold	0.8296	0.8960	0.9365	0.2678	0.2939	0.3252	0.7211	0.7403	0.7605
Test with EXPA	0.0188	0.0461	0.0808	0.0198	0.0382	0.0684	0.0192	0.0369	0.0674
EXPA adv cold	0.0036	0.0057	0.0155	0.0150	0.0392	0.0904	0.0646	0.1284	0.2163
test with c-SEMA	0.0187	0.0461	0.0807	0.0198	0.0384	0.0685	0.0194	0.0371	0.0677
c-SEMA adv cold	0.0017	0.0071	0.0269	0.0027	0.0088	0.0274	0.0181	0.0572	0.1314
Tradesy.com									
Original test	0.0338	0.0561	0.0869	0.0241	0.0439	0.0789	0.0234	0.0446	0.0819
Cooperative cold	0.0003	0.0013	0.0046	0.0022	0.0045	0.0096	0.0011	0.0026	0.0059
Test with INSA	0.0284	0.0526	0.0844	0.0224	0.0406	0.0707	0.0228	0.0439	0.0812
INSA adv cold	0.9399	0.9710	0.9843	0.0783	0.0965	0.1193	0.2711	0.2999	0.3326
Test with EXPA	0.0338	0.0561	0.0869	0.0228	0.0410	0.0710	0.0232	0.0445	0.0818
EXPA adv cold	0.0002	0.0003	0.0003	0.0048	0.0109	0.0234	0.0384	0.0602	0.0915
Test with c-SEMA	0.0338	0.0560	0.0870	0.0227	0.0410	0.0710	0.0234	0.0446	0.0819
c-SEMA adv cold	0.0000	0.0000	0.0000	0.0048	0.0104	0.0218	0.0005	0.0016	0.0048

Table 6. Change in average HR@5 before and after AIP attacks: Cold items (attack is successful HR@5 rises) and test items (successful attacks cause a drop in HR@5).

	Amazon Men			Tradesy.com		
	AlexRank	VBPR	DVBPR	AlexRank	VBPR	DVBPR
INSA adv cold vs. cooperative cold	$\uparrow 0.8109$	$\uparrow 0.2661$	$\uparrow 0.7201$	$\uparrow 0.939$	$\uparrow 0.0761$	$\uparrow 0.2700$
EXPA adv cold vs. cooperative cold	$\uparrow 0.0025$	$\uparrow 0.0133$	$\uparrow 0.0636$	$\downarrow 0.0001$	$\uparrow 0.0026$	$\uparrow 0.0373$
c-SEMA adv cold vs. cooperative cold	$\uparrow 0.0006$	$\uparrow 0.0010$	$\uparrow 0.0171$	$\downarrow 0.0003$	$\uparrow 0.0026$	$\downarrow 0.0006$
INSA test vs. original test	$\downarrow 0.0047$	$\downarrow 0.0001$	$\downarrow 0.0025$	$\downarrow 0.0054$	$\downarrow 0.0017$	$\downarrow 0.0006$
EXPA test vs. original test	$\uparrow 0.0001$	$\uparrow 0.0007$	$\downarrow 0.0003$	0.0000	$\downarrow 0.0013$	$\downarrow 0.0002$
c-SEMA test vs. original test	0.0000	$\uparrow 0.0007$	$\downarrow 0.0001$	0.0000	$\downarrow 0.0014$	0.0000

Note that the different performance of EXPA and c-SEMA on Amazon Men and Tradesy.com is not caused by the adversarial attack itself, rather the selection of the hook item. In Tradesy.com, the HR@N for the selected hook item (which is a gray coat) is low, so after EXPA or c-SEMA, the rank does not increase dramatically.

Table 6 focuses on the change in mean average hit rate $\Delta_{\text{cold}}^{\text{HR@N}}$ and average hit rate change $\Delta_{\text{test}}^{\text{HR@N}}$, so that the magnitude of the change can be appreciated directly. INSA has the largest positive effect on the adversarial item and largest negative effect on the test items. Again, the c-SEMA attack is surprisingly effective, given the minimal knowledge it involves. Remember that the recommender system platforms we are concerned about are enormous, and even a small boost in average rank of the magnitude of that afforded by c-SEMA could translate in to a substantial increase in interactions and profit.

Figure 4 shows a 2-D visualization of the image space defined by the DVBPR item embeddings. It allows us to directly observe the influences of different AIP attacks. The position of the original image (a cooperative image) is shown by ①. We can see that it is positioned next to items with which it is visually similar. The attacks move this image to the other positions. The hook item is a pair of jeans. We can see that EXPA, c-SEMA, and n-SEMA push the cold item to a cluster related to the hook item. Note that it is difficult to reason about the position of INSA, since it is optimized with respect to user embeddings.

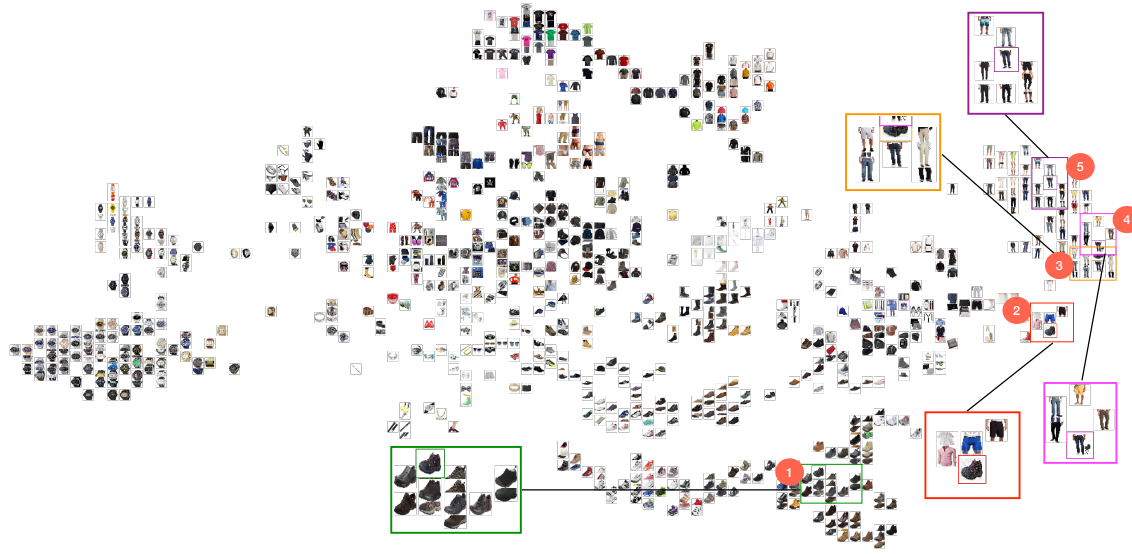


Fig. 4. t-SNE [21] 2-D visualization of item embedding by pre-trained DVBPR model (#factors = 100) for randomly selected 1000 items in Amazon Men data set, cooperative item (①) embedding and its corresponding adversarial item embedding. Attacks include generated images by INSA (②), EXPA (③), c-SEMA(④) and n-SEMA(⑤).

5.3.2 Influence of hyper-parameters. We mount attacks to models with reduced embedding length. We conduct experiments for different numbers of factors for VBPR in {20, 50, 100}, and for DVBPR {10, 30, 50, 100}. It is found that the recommender system with smaller embedding length is more susceptible to attacks.

We also investigate how the magnitude of ϵ influences the adversarial strength, we carry out experiments with ϵ in {4, 8, 26, 32} for INSA and EXPA. We found that increasing ϵ from 4 to 32 leads to improved adversarial effects, but large perturbation size is not necessary in most cases for a successful attack. In other words, the artifacts visible in Figure 3 (a) and (b) represent a worse-case scenario. Approaches that make adversarial images large yet imperceptible [38] can also be incorporated to boost AIP attacks and further eliminate artifacts.

5.4 Defense

In the computer vision literature, simple defenses have been shown to be effective against adversarial images that cause neural classifiers to misclassify [9, 12, 14, 35]. Here, we evaluated two common defenses: JPEG compression and bit depth reduction in order to test whether they are effective against AIP attacks. These are known to be able to erase the effect of image perturbations, which are used by INSA and EXPA. We carried out an evaluation by applying progressively stronger versions of the defense to adversarial images. We used a 100-item subset of our larger test set. We do not evaluate SEMA, since the semantic attack does not involve perturbations and if these defenses would destroy the effectiveness of SEMA they would also destroy the usefulness of cooperative images.

In Table 7, we visualize the level of strength of defense that must be applied to the adversarial image in order for its rank to be lowered to the average HR@5 of a cooperative image. If the defenses presented a surefire defense against adversarial item images (as they are for many classification algorithms), then we would expect the \blacktriangle and \star to appear consistently to the far left in the boxes. This is clearly not the case. We see in Table 7 that INSA is more difficult to defeat

Table 7. Visualization of the level at which a defense is successful at lowering the HR@5 of an adversarial cold-start item equal or less the average HR@5 of a cooperative cold-start item. For JPEG compression, levels are specified as compression percents and for Bit depth reduction levels are specified as number of bits with which the image is encoded. (▲: Amazon.com; ★: Tradesy.com)

		JPEG compression					Bit depth reduction					
		90	70	50	30	10	7	6	5	4	3	2
AlexRank	INSA											
	EXPA										▲	
VBPR	INSA											
	EXPA	▲★									▲★	
DVBPR	INSA						★					
	EXPA					▲						▲★

than EXPA, which is expected because it leverages insider knowledge of the recommender system. However, EXPA is clearly not easy to beat across the board. Our overall conclusion is that it is non-trivial to defeat INSA and EXPA in a cold start situation and that the recommender research community must devote more effort to solving the problem.

It is important to note that this test is a strong one. If these defenses would be applied in practice, they would need to be applied to all images and not just adversarial images. Image content becomes indistinguishable as compression increases, and an image 10% the size of the original image or encoded with only 2-3 bits can be expected to contain little to no item information.

Another possible approach would be to train a gateway classifier that would screen for adversarial images at the moment that merchants upload them to the recommender system platform. It is clear that for SEMA such a classifier would be difficult to build, since SEMA attacks are created in a natural manner and are indistinguishable from cooperative images. For INSA and EXPA, a gateway filter could be built if the exact specifications of the adversarial attack, including the parameter settings were known. The number of possible variants on INSA and EXPA attacks is so large, however, that it would be prohibitive to try to guess the parameters.

6 CONCLUSION AND OUTLOOK

This paper has investigated the vulnerabilities at the core of Top-N recommenders that use images to address cold start. We have shown that Adversarial Item Promotion (AIP) attacks allow unscrupulous merchants to artificially raise the rank of their products when a visually-aware recommender system is used for candidate ranking. The evidence from our investigation leads us to conclude that AIP attacks are a potential threat with clear practical implications. Our work reveals that the promise of hybrid recommender systems to provide a higher degree of robustness [24] is not an absolute, and that we must proceed with caution when using images to address cold start.

Future work must develop effective defenses against AIP attacks. One approach, already mentioned above, is to use a gateway classifier to flag adversarial images at the moment merchants upload them. Unfortunately, AIP attacks can bypass such a classifier by constructing new loss functions [6]. Another approach is adversarial training, which has proved an effective way to increase robustness against adversarial examples [22]. This solution requires vast computational resources and the resulting system achieves robustness at the risk of sacrificing the original performance.

Future work must look at the impact of multipliers. If a single item has multiple descriptive images, attacks are more likely to go unnoticed, in particular semantic attacks that require no perturbations. Further, multiple merchants (or fake merchant profiles) could collaborate in a collusion attack.

Finally, we note that although, here, we have focused on e-commerce, entertainment recommender systems are vulnerable: an adversarial signal could be embedded into a thumbnail or the content itself. In sum, AIP attacks constitute an important, practical risk of using images in recommender systems and serious challenges remain to be addressed.

REFERENCES

- [1] Marco Barreno, Blaine Nelson, Anthony D Joseph, and J Doug Tygar. 2010. The security of machine learning. *Machine Learning* 81, 2 (2010), 121–148.
- [2] Alexandra Berzon, Shane Shifflett, and Justin Scheck. 2019. Amazon Has Ceded Control of Its Site. The Result: Thousands of Banned, Unsafe or Mislabeled Products. <https://www.wsj.com/articles/amazon-has-ceded-control-of-its-site-the-result-thousands-of-banned-unsafe-or-mislabeled-products-11566564990>. Accessed: 2020-06-01.
- [3] Battista Biggio, Iginio Corona, Davide Maiorca, Blaine Nelson, Nedom Šrđić, Pavel Laskov, Giorgio Giacinto, and Fabio Roli. 2013. Evasion attacks against machine learning at test time. In *Joint European Conference on Machine Learning and Knowledge Discovery in Databases (ECML-PKDD)*. Springer, 387–402.
- [4] Christian Bracher, Sebastian Heinz, and Roland Vollgraf. 2016. Fashion DNA: Merging content and sales data for recommendation and article mapping. In *KDD Fashion Workshop*.
- [5] Robin Burke, Michael P O’Mahony, and Neil J Hurley. 2015. Robust collaborative recommendation. In *Recommender systems handbook*. Springer, 961–995.
- [6] Nicholas Carlini and David Wagner. 2017. Adversarial examples are not easily detected: Bypassing ten detection methods. In *ACM Workshop on Artificial Intelligence and Security*. 3–14.
- [7] Nicholas Carlini and David Wagner. 2018. Audio adversarial examples: Targeted attacks on speech-to-text. In *2018 IEEE Security and Privacy Workshops (SPW)*. IEEE, 1–7.
- [8] Konstantina Christakopoulou and Arindam Banerjee. 2019. Adversarial attacks on an oblivious recommender. In *ACM Conference on Recommender Systems (RecSys)*. 322–330.
- [9] Nilaksh Das, Madhuri Shanbhogue, Shang-Tse Chen, Fred Hohman, Siwei Li, Li Chen, Michael E Kounavis, and Duen Horng Chau. 2018. Shield: Fast, practical defense and vaccination for deep learning using jpeg compression. In *ACM SIGKDD International Conference on Knowledge Discovery and Data Mining (KDD)*. 196–204.
- [10] James Davidson, Benjamin Liebald, Junning Liu, Palash Nandy, Taylor Van Vleet, Ullas Gargi, Sujoy Gupta, Yu He, Mike Lambert, Blake Livingston, et al. 2010. The YouTube video recommendation system. In *ACM Conference on Recommender Systems (RecSys)*. 293–296.
- [11] Tommaso Di Noia, Daniele Malitesta, and Felice Antonio Merri. 2020. TAaMR: Targeted adversarial attack against multimedia recommender systems. In *International Workshop on Dependable and Secure Machine Learning*.
- [12] Gintare Karolina Dziugaite, Zoubin Ghahramani, and Daniel M Roy. 2016. A study of the effect of jpg compression on adversarial images. In *International Society for Bayesian Analysis*.
- [13] João Gomes. 2017. Boosting recommender systems with deep learning. In *ACM Conference on Recommender Systems (RecSys)*. 344–344.
- [14] Chuan Guo, Mayank Rana, Moustapha Cisse, and Laurens Van Der Maaten. 2018. Countering adversarial images using input transformations. *International Conference on Learning Representations (ICLR)*.
- [15] Ruining He and Julian McAuley. 2016. VBPR: Visual bayesian personalized ranking from implicit feedback. In *AAAI Conference on Artificial Intelligence (AAAI)*.
- [16] Vignesh Jagadeesh, Robinson Piramuthu, Anurag Bhardwaj, Wei Di, and Neel Sundaresan. 2014. Large scale visual recommendations from street fashion images. In *ACM SIGKDD International Conference on Knowledge Discovery and Data Mining (KDD)*. 1925–1934.
- [17] Yannis Kalantidis, Lyndon Kennedy, and Li-Jia Li. 2013. Getting the look: Clothing recognition and segmentation for automatic product suggestions in everyday photos. In *ACM conference on International conference on multimedia retrieval (ICMR)*. 105–112.
- [18] Wang-Cheng Kang, Chen Fang, Zhaowen Wang, and Julian McAuley. 2017. Visually-aware fashion recommendation and design with generative image models. In *IEEE International Conference on Data Mining (ICDM)*. IEEE, 207–216.
- [19] Shyong K Lam and John Riedl. 2004. Shilling recommender systems for fun and profit. In *International conference on World Wide Web (WWW)*. 393–402.
- [20] Joonseok Lee and Sami Abu-El-Haija. 2017. Large-scale content-only video recommendation. In *IEEE International Conference on Computer Vision Workshops (ICCVW)*. 987–995.
- [21] Laurens van der Maaten and Geoffrey Hinton. 2008. Visualizing data using t-SNE. *Journal of machine learning research* 9, Nov (2008), 2579–2605.
- [22] Aleksander Madry, Aleksandar Makelov, Ludwig Schmidt, Dimitris Tsipras, and Adrian Vladu. 2018. Towards deep learning models resistant to adversarial attacks. In *International Conference on Learning Representations (ICLR)*.
- [23] Julian McAuley, Christopher Targett, Qinfeng Shi, and Anton Van Den Hengel. 2015. Image-based recommendations on styles and substitutes. In *International ACM SIGIR Conference on Research and Development in Information Retrieval (SIGIR)*. 43–52.
- [24] Bamshad Mobasher, Robin Burke, Runa Bhaumik, and Chad Williams. 2007. Toward trustworthy recommender systems: An analysis of attack models and algorithm robustness. *ACM Transactions on Internet Technology (TOIT)* 7, 4 (2007), 23.
- [25] Michael P O’Mahony, Neil J Hurley, and Guenole CM Silvestre. 2002. Promoting recommendations: An attack on collaborative filtering. In *International Conference on Database and Expert Systems Applications*. Springer, 494–503.
- [26] Adam Paszke, Sam Gross, Soumith Chintala, Gregory Chanan, Edward Yang, Zachary DeVito, Zeming Lin, Alban Desmaison, Luca Antiga, and Adam Lerer. 2017. Automatic differentiation in PyTorch. In *NIPS Autodiff Workshop*.

- [27] Bobby Prévost, Jonathan Laflamme Janssen, Jaime R Camacaro, and Carolina Bessega. 2018. Deep inventory time translation to improve recommendations for real-world retail. In *ACM Conference on Recommender Systems (RecSys)*. 195–199.
- [28] Steffen Rendle, Christoph Freudenthaler, Zeno Gantner, and Lars Schmidt-Thieme. 2012. BPR: Bayesian personalized ranking from implicit feedback. In *Conference on Uncertainty in Artificial Intelligence (UAI)*.
- [29] Sara Sabour, Yanshuai Cao, Fartash Faghri, and David J Fleet. 2016. Adversarial manipulation of deep representations. *International Conference on Learning Representations (ICLR)*.
- [30] Sandhya Sachidanandan, Richard Luong, and Emil S Joergensen. 2019. Designer-driven add-to-cart recommendations. In *ACM Conference on Recommender Systems (RecSys)*. 525–525.
- [31] Edgar Simo-Serra, Sanja Fidler, Francesc Moreno-Noguer, and Raquel Urtasun. 2015. Neuroaesthetics in fashion: Modeling the perception of fashionability. In *IEEE Conference on Computer Vision and Pattern Recognition (CVPR)*. 869–877.
- [32] Christian Szegedy, Wojciech Zaremba, Ilya Sutskever, Joan Bruna, Dumitru Erhan, Ian Goodfellow, and Rob Fergus. 2014. Intriguing properties of neural networks. In *International Conference on Learning Representations (ICLR)*.
- [33] Jinhui Tang, Xiaoyu Du, Xiangnan He, Fajie Yuan, Qi Tian, and Tat-Seng Chua. 2020. Adversarial training towards robust multimedia recommender system. *IEEE Transactions on Knowledge and Data Engineering (TKDE)* 32, 5 (2020), 855–867.
- [34] Jizhe Wang, Pipei Huang, Huan Zhao, Zhibo Zhang, Binqiang Zhao, and Dik Lun Lee. 2018. Billion-scale commodity embedding for e-commerce recommendation in alibaba. In *ACM SIGKDD International Conference on Knowledge Discovery and Data Mining (KDD)*. 839–848.
- [35] Weilin Xu, David Evans, and Yanjun Qi. 2017. Feature squeezing: Detecting adversarial examples in deep neural networks. In *Network and Distributed Systems Security Symposium (NDSS)*.
- [36] Fuzheng Zhang, Nicholas Jing Yuan, Defu Lian, Xing Xie, and Wei-Ying Ma. 2016. Collaborative knowledge base embedding for recommender systems. In *ACM SIGKDD International Conference on Knowledge Discovery and Data Mining (KDD)*. 353–362.
- [37] Yongfeng Zhang, Qingyao Ai, Xu Chen, and W Bruce Croft. 2017. Joint representation learning for top-n recommendation with heterogeneous information sources. In *ACM Conference on Information and Knowledge Management (CIKM)*. 1449–1458.
- [38] Zhengyu Zhao, Zhuoran Liu, and Martha Larson. 2020. Towards large yet imperceptible adversarial image perturbations with perceptual color distance. In *IEEE Conference on Computer Vision and Pattern Recognition (CVPR)*.